Inorg. Chem. **2004**, *43*, 6455–6463

Structural Characterization and Electronic Properties Determination by High-Field and High-Frequency EPR of a Series of Five-Coordinated Mn(II) Complexes

Claire Mantel,[†,‡] Carole Baffert,[‡] Isabel Romero,[‡] Alain Deronzier,[‡] Jacques Pécaut,[§] Marie-Noëlle Collomb,*[,‡] and Carole Duboc*[,†]

Grenoble High Magnetic Field Laboratory, CNRS-MPI, BP 166, 38042 Grenoble Cedex 9, Laboratoire d'Electrochimie Organique et de Photochimie Rédox, CNRS UMR 5630, Institut de Chimie Moléculaire de Grenoble, FR CNRS 2607, Université Joseph Fourier, BP 53, 38041 Grenoble Cedex 9, and DRFMC-service de chimie inorganique et biologique, laboratoire coordination et chiralité, CEA-Grenoble, 38054 Grenoble Cedex, France

Received March 16, 2004

The isolation, structural characterization, and electronic properties of a series of high-spin mononuclear five-coordinated Mn(II) complexes, [Mn(terpy)$(X)_2$] (terpy = 2, 2′:6′,2″-terpyridine; X = I^- (**1**), Br^- (**2**), Cl^- (**3**), or SCN^- (**4**)), are reported. The X-ray structures of the complexes reveal that the manganese ion lies in the center of a distorted trigonal bipyramid for complexes **1**, **2**, and **4**, while complex **3** is better described as a distorted square pyramid. The electronic properties of **1**–**4** were investigated by high-field and high-frequency EPR spectroscopy (HF-EPR) performed between 5 and 30 K. The powder HF-EPR spectra have been recorded in high-field-limit conditions (95–285 GHz) ($D \ll g\beta B$). The spectra are thus simplified, allowing an easy interpretation of the experimental data and an accurate determination of the spin Hamiltonian parameters. The magnitude of D varies between 0.26 and 1.00 cm^{-1} with the nature of the anionic ligand. Thanks to low-temperature EPR experiments, the sign of D was unambiguously determined. D is positive for the iodo and bromo complexes and negative for the chloro and thiocyano ones. A structural correlation is proposed. Each complex is characterized by a significant rhombicity with E/D values between 0.17 and 0.29, reflecting the distorted geometry observed around the manganese. Finally, we compared the spin Hamiltonian parameters of our five-coordinated complexes and those previously reported for other analogous series of dihalo four- and six-coordinated complexes. The effect of the coordination number and of the geometry of the Mn(II) complexes on the spin Hamiltonian parameters is discussed.

Introduction

High-spin mononuclear Mn(II) complexes are largely investigated since they are of importance in several fields such as materials chemistry,[1] catalysis,[2] or biochemistry.[3] The Mn(II) ion is often used as a building element in nanomagnets[1] as well as for the development of catalysts especially for oxidation reactions.[2] Mononuclear Mn(II) complexes are also found in a number of metalloenzymes as active sites.[3]

* Authors to whom correspondence should be addressed. Fax: 33 4 76 85 56 10 (C.B.); 33 4 76 51 42 67 (M.-N.C.). E-mail: duboc@grenoble.cnrs.fr (C.B.) Marie-Noelle.Collomb@ujf-grenoble.fr (M.-N.C.).

† CNRS-MPI.

‡ Université Joseph Fourier.

§ CEA Grenoble.

(1) (a) Sanudo, E. C.; Grillo, V. A.; Knapp, M. J.; Bollinger, J. C.; Huffman, J. C.; Hendrickson, D. N.; Christou, G. *Inorg. Chem.* **2002**, *41*, 2441. (b) Yoo, J.; Yamaguchi, A.; Nakano, M.; Krzystek, J.; Streib, W. E.; Brunel, L.-C.; Ishimoto, H.; Christou, G.; Hendrikson, D. N. *Inorg. Chem*. **2001**, *40*, 4604.

(2) (a) Deroche, A.; Morgenstern-Baradau, I.; Cesario, M.; Guilhem, J.; Keita, B.; Nadjo, L.; Houée-Levin, C. *J. Am. Chem. Soc.* **1996**, *118*, 4567. (b) Shimanovich, R.; Hannah, S.; Lynch, V.; Gerasimchuk, N.; Mody, T. D.; Magda, D.; Sessler, J.; Groves, J. T. *J. Am. Chem. Soc.* **2001**, *123*, 3613. (c) Pan, J.-F.; Chen, K. *J. Mol. Catal. A* **2001**, *176*, 19. (d) Wieprecht, T.; Xia, J.; Heinz, U.; Dannacher, J.; Schlingloff, G. *J. Mol. Catal. A* **2003**, *203*, 113 and references therein.

(3) (a) Bernat, B. A.; Laughlin, L. T.; Armstrong, R. N. *Biochemistry* **1999**, *38*, 7462. (b) Requena, L.; Bornemann, S. *Biochem. J.* **1999**, *343*, 185. (c) Boldt, Y. R.; Whiting, A. K.; Wagner, M. L.; Sadowsky, M. J.; Que, L.; Wackett, L. P. *Biochemistry* **1997**, *36*, 2147. (d) Whittaker, M. M.; Whittaker, J. W. *Biochemistry* **1997**, *36*, 8923. (e) Schwartz, A. L.; Yikilmaz, E.; Vance, C. K.; Vathyam, S.; Koder, R. L.; Miller, A.-F. *J. Inorg. Biochem.* **2000**, *80*, 247. (f) Bogumil, R.; Kappl, R.; Hüttermann, J.; Witzel, H. *Biochemistry* **1997**, *36*, 2345. (g) Smoukov, S. K.; Telser, J.; Bernat, B. A.; Rife, C. L.; Armstrong, R. N.; Hoffman, B. M. *J. Am. Chem. Soc.* **2002**, *124*, 2318.

10.1021/ic049650k CCC: $27.50
Published on Web 09/09/2004

The reactivity of the Mn(II) complexes is correlated with their geometry and thus their electronic structure. One of the best techniques to elucidate the electronic properties of such compounds is the EPR spectroscopy.

In this context, we focus our attention on developing new mononuclear Mn(II) complexes to investigate in detail their electronic properties by using high-field and high-frequency EPR spectroscopy (HF-EPR). High-spin Mn(II) ion ($3d^5$) is characterized by a fundamental electronic spin $S = 5/2$ and a nuclear spin $I = 5/2$ (^{55}Mn, 100%). Its electronic properties are described by the following spin Hamiltonian:

$$H = \beta BgS + IAS + D[S_z^2 - (1/3)S(S+1)] + E(S_x^2 - S_y^2) \quad (1)$$

The first two terms represent the electronic Zeeman and the electron nuclear hyperfine interactions, respectively, whereas the last two terms define the zero-field splitting (zfs) interaction with D and E gauging the axial and the rhombic parts.

The majority of EPR studies performed on mononuclear Mn(II)-containing enzymes[3] have been done at the X-band (9.4 GHz) or Q-band (35 GHz), as well as several studies on inorganic complexes, in solution.[4] In these highly diluted conditions, when D is much smaller than the microwave quantum used by the spectrometer, the typical EPR spectra exhibit a unique feature (sextuplet) centered at around $g = 2$. This sextuplet is associated with the $|5/2, -1/2\rangle \rightarrow |5/2, +1/2\rangle$ transition, which is split because of the interaction between the electronic and nuclear spins of Mn(II). Two subsequent lines of the sextuplet are usually separated by about 80−100 G. The shape of the sextuplet depends on the magnitude of the different spin Hamiltonian terms. It becomes more complicated with additional lines and then appears as a multiplet when the zfs terms increase until making the EPR spectra difficult to interpret and in some cases uninterpretable. HF-EPR spectroscopy have been proven to be a useful tool to study Mn(II)-containing protein samples.[5] Indeed, simplified EPR spectra are obtained when higher microwave frequencies such as 95 or even 285 GHz are used. In these high-field conditions ($D \ll g\beta B$), EPR spectra recorded, for example, on the manganese superoxide dismutase in the native state, exhibit a simplified multiplet from which the spin Hamiltonian parameters have been precisely determined.[5a,b] The four other transitions ($|5/2, -5/2\rangle \rightarrow |5/2, -3/2\rangle$, $|5/2, -3/2\rangle \rightarrow |5/2, -1/2\rangle$, $|5/2, +1/2\rangle \rightarrow |5/2, +3/2\rangle$, $|5/2, +3/2\rangle \rightarrow |5/2, +5/2\rangle$) expected along each direction (x, y, and z) for an $S = 5/2$ paramagnet are usually not observed when the experiments are performed in diluted conditions since their intensity is too weak.

X-band and Q-band EPR studies have also been performed on powder or crystal samples of synthetic mononuclear Mn(II) complexes.[6] For systems with small D, some or all expected transitions are observed on the EPR spectra, and their analysis is feasible. Otherwise, when D is larger or comparable to the energy provided by the EPR spectrometer, the spectra become more complicated. Nevertheless, the determination of the spin Hamiltonian parameters by X-band EPR has been achieved in the case of the manganese-doped complexes $[Mn(N_2H_4)_2(X)_2]$[6e] and $[Mn(pyr)_4(X)_2]$[6f] (pyr = pyridine; X = I^-, Br^-, Cl^-, SCN^-), even if some of these complexes present a large D. Thanks to the magnetic dilution, the X-band EPR spectra show several transitions split by hyperfine interactions that allow the analysis of the spectra.

However, for powder samples of manganese(II) complexes with large a D value, the use of HF-EPR spectroscopy is necessary to precisely determine the spin Hamiltonian parameters. Indeed, when high-field-limit conditions are reached, transitions between two Zeeman levels occur by following the rule $\Delta M_s = \pm 1$, and the two levels are separated by a characteristic field difference. Furthermore, a multifrequency EPR study allows the unambiguous determination of the spin Hamiltonian parameters since the same set of parameters simulates spectra recorded at all frequencies and temperatures.

To our knowledge, only three HF-EPR papers on powder mononuclear Mn(II) samples have been published.[7] The following series of dihalo complexes have been studied: $[Mn(PPhO)_2(X)_2]$, $[Mn(phen)_2(X)_2]$, $[Mn(pic)_2(X)_2]$, and $[Mn(pyr)_4(X)_2]$ (PPhO = triphenylphosphine oxide; phen = *o*-phenanthroline; pic = γ-picoline; X = I^-, Br^-, Cl^-). The PPhO complexes have a distorted tetrahedral geometry, while those with phen, pic, and pyr show an octahedral geometry. HF-EPR spectra have been recorded, and the spin Hamiltonian parameters have been determined. A good correlation was found between the ligand field strength of the anion and the magnitude of D. However, the sign of D was not determined since the HF-EPR experiments have been performed at room temperature.

In this work, we focus our attention on five-coordinated Mn(II) complexes which are still rarely described. Even if Mn(II) leads to a wide range of coordination numbers (2−

(4) (a) Mikuriy, M.; Hatano, Y.; Asato, E. *Bull. Chem. Soc. Jpn*. **1997**, *70*, 2495. (b) Warzeska, S. T.; Micciche, F.; Mimmi, M. C.; Bouwman, E.; Kooijman, H.; Spek, A. L., Reedijk, J. *J. Chem. Soc., Dalton Trans*. **2001**, 3507.

(5) (a) Un, S.; Tabares, L. C.; Cortez, N.; Hiraoka, B. Y.; Yamakura, F. *J. Am. Chem. Soc*. **2004**, *126*, 2720−2726. (b) Un, S.; Dorlet, P.; Voyard, G.; Tabares, L. C.; Cortez, N. *J. Am. Chem. Soc.* **2001**, *123*, 10123. (c) Carmieli, R.; Manikandan, P.; Epel, B.; Kalb, A. J.; Schnegg, A.; Savitsky, A.; Möbius, K.; Goldfarb, D. *Biochemistry* **2003**, *42*, 7863. (d) Buy, C.; Girault, G.; Zimmermann, J.-L. *Biochemistry* **1996**, *35*, 9880−9891. (e) Käss, H.; MacMillan, F.; Ludwig, B.; Prisner, T. *J. Phys. Chem. B* **2000**, *104*, 5362−5371.

(6) (a) Gahan, L. R.; Grillo, V. A.; Hambley, T. W.; Hanson, G. R.; Hawkins, C. J.; Proudfoot, E. M.; Moubaraki, B.; Murray, K. S.; Wang, D. *Inorg. Chem.* **1996**, *35*, 1039. (b) Bucher, C.; Duval, E.; Barbe, J.-M.; Verpeaux, J.-N.; Amatore, C.; Guillard, R.; Le Pape, L.; Latour, J.-M.; Dahaoui, S.; Lecomte, C. *Inorg. Chem.* **2001**, *40*, 5722. (c) Meirovitch, E.; Luz, Z.; Kalb, J. *J. Am. Chem. Soc.* **1974**, *96*, 7538. (d) Dowsing, R. D.; Gibson, J. F.; Goodgame, D. M. L.; Goodgame, M.; Hayward, P. J. *J. Chem. Soc. A* **1969**, 1242. (e) Birdy, R. B.; Goodgame, M. *Inorg. Chim. Acta* **1981**, *50*, 183. (f) Jacobsen, C. J. H.; Pedersen, E.; Villadsen, J.; Weihe, H. *Inorg. Chem.* **1993**, *32*, 1216. (g) Vivien, D.; Gibson, J. F. *J. Chem. Soc., Faraday Trans. 2* **1975**, 1640. (h) Kosky, C. A.; Gayda, J.-P.; Gibson, J. F.; Jones, S. F.; Williams, D. J. *Inorg. Chem.* **1982**, *21*, 3173 and references therein.

(7) (a) Lynch, W. B.; Boorse, R. S.; Freed, J. H. *J. Am. Chem. Soc.* **1993**, *115*, 10909. (b) Wood, R. M.; Stucker, D. M.; Jones, L. M.; Lynch, W. B.; Misra, S. K.; Freed, J. H. *Inorg. Chem.* **1999**, *38*, 5384. (c) Goodgame, D. M. L.; Mkami, H. E.; Smith, G. M.; Zhao, J. P.; McInnes, E. J. L. *J. Chem. Soc., Dalton Trans*. **2003**, 34.

8), the most common coordination number of structurally characterized Mn(II) complexes is 6.[8] In this paper, we present the synthesis and the structural characterization of a series of four complexes, $[Mn(terpy)(X)_2]$ (terpy = 2,2′:6′,2″-terpyridine; X = I^- (**1**), Br^- (**2**), Cl^- (**3**), SCN^- (**4**)). Complexes **1**−**3** were isolated in the 1960s using other synthetic methods.[9] Compounds **1** and **2** have not been structurally characterized until now, while the X-ray structure of **3** has been recently published, in parallel with our work.[10] In this study, the electronic properties of complexes **1**−**4** are investigated by HF-EPR (95−285 GHz) between 5 and 30 K and the spin Hamiltonian parameters determined. Furthermore, we compare our results with those previously reported for an analogous series of dihalo four- and six-coordinated complexes. Finally, we also show the importance of recording spectra at low temperature to unambiguously determine the sign of *D*, and we are able to propose a good correlation between the sign of *D* and the structural properties of complexes **1**−**4**.

Experimental Section

The ligand 2,2′:6′,2″-terpyridine (terpy) and solvents were purchased from Aldrich and used as received. Compounds **1**−**3** have been previously isolated.[9,10] We used the following new synthetic methods to isolate these compounds.

Synthesis of [Mn(terpy)(I)$_2$] (1). To a stirred solution of terpy (50 mg, 0.214 mmol) in 3 mL of methanol was added $Mn(CH_3CO_2)_2 \cdot 4H_2O$ (52.4 mg, 0.214 mmol). The resulting yellow solution was stirred at room temperature for 10 min and filtered. A saturated solution of Bu_4NI in 5 mL of methanol was added to the yellow solution. Yellow crystals of **1** were grown by slow diffusion of dichloromethane in this solution. Yield: 0.066 g (57%). Anal. Calcd for complex **1** ($C_{15}H_{11}MnN_3I_2$ (542.01)): C, 45.42; H, 3.05; N, 10.59. Found: C, 45.40; H, 2.97; N, 10.58. IR (cm^{-1}, KBr): ν = 2920(m), 1593(m), 1573(s), 1557(w), 1475(m), 1452(s), 1435(s), 1314(m), 1250(m), 1159(m), 1013(s), 776(s), 649(m), 403(m).

Synthesis of [Mn(terpy)(Br)$_2$] (2). To a stirred solution of terpy (100 mg, 0.428 mmol) in 2 mL of methanol was added $MnBr_2$ in 2 mL of water (92 mg, 0.428 mmol). The resulting solution was filtered, and after several days of slow evaporation at room temperature, orange crystals of **2** were obtained. Yield: 0.114 g (56%). Anal. Calcd for complex **2** ($C_{15}H_{11}MnN_3Br_2$ (448.03)): C, 40.21; H, 2.47; N, 9.38. Found: C, 40.07; H, 2.47; N, 9.41. IR (cm^{-1}, KBr): ν = 3042(m), 1593(s), 1573(m), 1561(m), 1474(m), 1452(s), 1316(m), 1297(m), 1252(m), 1159(m), 1014(s), 776(s), 650(m), 637(m), 402(m).

Synthesis of [Mn(terpy)(Cl)$_2$] (3). Method A. To a stirred solution of terpy (116.6 mg, 0.5 mmol) in 15 mL of methanol was added anhydrous $MnCl_2$ in 2 mL of methanol (63 mg, 0.5 mmol). The mixture was stirred at room temperature for 15 min. The yellow precipitate obtained was then filtered off, and the filtrate was concentrated by rotary evaporation to give more of the yellow solid. The combined solids were washed with a small amount of cold methanol and dried in vacuo. Yield: 0.095 g (53%). The yellow solid was redissolved in 100 mL of methanol and left to evaporate at room temperature. After one month, orange crystals of **3**, suitable for X-ray analysis, formed as yellow plates. They were filtered and washed with a small amount of methanol. Yield: 0.056 g (31%). Anal. Calcd for complex **3**·H_2O ($C_{15}H_{13}MnN_3O_1Cl_2$ (376.9)): C, 48.94; H, 3.29; N, 11.41. Found: C, 48.88; H, 3.12; N, 11.59. IR (cm^{-1}, KBr): ν = 3052(m), 1593(s), 1574(m), 1558(m), 1494(s), 1473(m), 1449(s), 1435(m), 1403(w), 1313(m), 1294(w), 1247(m), 1192(w), 1158(m), 1013(s), 769(vs), 658(w), 650(m), 638(m), 511(w), 426(w), 410(w).

Method B. To an aqueous solution (2 mL) of anhydrous $MnCl_2$ (0.0269 g, 0.214 mmol) was added with stirring an ethanol solution (2 mL) of terpy ligand (0.050 g, 0.214 mmol). The resulting yellow solution was stirred for 20 min and then filtered to remove any impurities. After slow evaporation of the filtrate solution for 2 days, a yellow microcrystalline precipitate of **3** was obtained. Yield: 0.058 g (75%). Slow evaporation of a methanol solution of this complex gave crystals identical to those obtained from method A.

Synthesis of [Mn(terpy)(SCN)$_2$] (4). To a stirred solution of terpy (50 mg, 0.214 mmol) in 3 mL of methanol was added $Mn(CH_3CO_2)_2 \cdot 4H_2O$ (52.4 mg, 0.214 mmol). The resulting yellow solution was stirred at room temperature for 10 min and filtered. A saturated solution of $Bu_4N(SCN)$ in 5 mL of methanol was added to the yellow solution, and a precipitate was formed. It was filtered, washed with a small amount of ethanol, and dried in vacuo. Yellow crystals of **4** were obtained at room temperature by slow evaporation of the yellow precipitate dissolved in a mixture of CH_3CN/DMSO (90/10). Yield: 0.082 g (95%). Anal. Calcd for complex **4** ($C_{17}H_{11}MnN_5S_2$ (404.37)): C, 50.50; H, 2.74; N, 17.32. Found: C, 50.74; H, 2.73; N, 17.31. IR (cm^{-1}, KBr): ν = 3059 (m), 2061 (vs), 1596 (s), 1574 (m), 1477 (m), 1452 (s), 1437 (m), 1313 (m), 1245 (m), 1164 (m), 1015 (m), 777 (s), 660 (m), 650 (m), 639 (m), 483 (m), 400 (m).

Physical Measurements. UV/vis spectra were recorded on a Cary 1 Varian spectrophotometer. IR spectra were obtained with a Perkin-Elmer Spectrum GX spectrophotometer, piloted by a Dell Optiplex GXa computer. Spectra were recorded with a solid sample at 1% in mass in a pellet of KBr. High-frequency and high-field EPR spectra were recorded on a laboratory-made spectrometer[11] using powder samples pressed into pellets to avoid preferential orientation of the crystallites in the strong magnetic field. Gunn diodes operating at 95 and 115 GHz and equipped with a second-, third-, fourth-, and fifth-harmonic generator were used as the radiation source. The magnetic field was produced by a superconducting magnet (0−12 T). The simulation of the HF-EPR spectra was performed using the SIM program written by H. Weihe.[6f] SIM performs a full-matrix diagonalization of the spin Hamiltonian. It is therefore adequate for spin systems with any value of the zfs parameter relative to the operating frequency. The program also takes into account the Boltzmann population factor in calculating transition intensities. Its detailed description is available on the Web site http://sophus.kiku.dk/software/epr/epr.html. We determined error bars via the following standard method: the error bar is defined as the difference between parameters yielding a resonance position at $H_0 + \Delta/2$ and $H_0 - \Delta/2$, H_0 being the peak position and Δ its full width at half-maximum. This procedure was repeated for each working frequency, and the largest error bar of all frequencies was chosen as the final error bar.

Crystal Structure Determination of the Complexes. Crystals of dimensions 0.1 × 0.1 × 0.4 mm for **1**, 0.2 × 0.3 × 0.5 mm for

(8) Cotton, F. A.; Wilkinson, G.; Murillo, A. C.; Bochmann, M. *Advanced Inorganic Chemistry*, 6th ed.; Wiley: New York, 1999; p 757.
(9) Judge, J. S.; Reiff, W. M.; Intille, G. M.; Ballway, P.; Baker, W. A. *J. Inorg. Nucl. Chem.* **1967**, *29*, 1711.
(10) Grirrane, A.; Pastor, A.; Alvarez, E.; Mealli, C.; Ienco, A.; Rosa, P.; Montilla, F.; Galindo, A. *Eur. J. Inorg. Chem.* **2004**, 707.
(11) (a) Barra, A.-L.; Brunel, L.-C.; Robert, J.-B. *Chem. Phys. Lett.* **1990**, *165*, 107. (b) Muller, F.; Hopkins, M.-A.; Coron, N.; Grynderg, M.; Brunel, L.-C.; Martinez, G. *Rev. Sci. Instrum.* **1989**, *60*, 3681.

Table 1. Principal Crystallographic Data of Complexes [Mn(terpy)$(I)_2$] (**1**), [Mn(terpy)$(Br)_2$] (**2**), [Mn(terpy)$(Cl)_2$] (**3**), and [Mn(terpy)$(SCN)_2$] (**4**)

	1	2	3	4
empirical formula	$C_{15}H_{11}I_2MnN_3$	$C_{15}H_{11}Br_2MnN_3$	$C_{15}H_{11}Cl_2MnN_3$	$C_{17}H_{11}S_2MnN_5$
fw	542.01	448.03	359.11	404.37
cryst syst	monoclinic	monoclinic	monoclinic	monoclinic
space group	*C*2/*c*	*C*2/*c*	*P*2(1)/*c*	*C*2/*c*
a (Å)	17.430(3)	17.119(6)	10.9854(5)	13.971(2)
b (Å)	9.8284(15)	9.439(3)	8.2509(4)	9.5551(16)
c (Å)	11.9284(19)	11.612(3)	16.3448(8)	14.485(2)
α (deg)	90	90	90	90
β (deg)	125.953(2)	126.44(2)	93.9660(10)	11.307(4)
γ (deg)	90	90	90	90
vol ($Å^3$)	1653.5(4)	1509.4(8)	1477.94(12)	1801.5(5)
T (K)	298(2)	298(2)	298(2)	298(2)
λ (Å)	0.71073	0.71073	0.71073	0.71073
density (mg m^{-3})	2.177	1.972	1.614	1.491
Z	4	4	4	4
μ (mm^{-1})	4.528	6.163	1.249	0.973
F(000)	1012	868	724	820
no. of reflns collected	3178	1659	9234	3474
R1[a]	0.1096	0.0670	0.0339	0.0869
wR2[b]	0.1770	0.1520	0.0787	0.0960

[a] $R1 = \sum||F_o| - |F_c||/\sum|F_o|$. [b] $wR2 = [(\sum w(|F_o| - |F_c|)^2/\sum wF_o^2)]^{1/2}$.

Table 2. Selected Bond Distances (Å) and Selected Angles (deg) for Complexes **1**, **2**, and **4**[a]

	1	2	4
Mn−X	2.7200(9)	2.5010(11)	2.062(3)
Mn−N(1)	2.240(6)	2.242(5)	2.241(3)
Mn−N(2)	2.233(7)	2.204(6)	2.192(3)
X−Mn−X#1	114.31(5)	116.08(6)	104.09(14)
X−Mn−N(1)	100.82(12)	98.17(13)	106.51(10)
X#1−Mn−N(1)#1			
X−Mn−N(1)#1	98.27(12)	100.63(12)	94.72(10)
X#1−Mn−N(1)			
X−Mn−N(2)	122.85(3)	121.96(3)	127.95(7)
N(1)−Mn−N(1)#1	144.4(3)	144.1(2)	145.33(13)
N(1)−Mn−N(2)	72.21(14)	72.03(12)	72.67(6)

[a] X = I for **1**, Br for **2**, and N_{SCN} for **4**. Symmetry transformations used to generate equivalent atoms (#1): $-x + 2, y, -z + 3/2$.

Table 3. Selected Bond Distances (Å) and Angles (deg) for Complex **3**

Mn−Cl(1)	2.3532(4)	Mn−N(2)	2.2099(11)
Mn−Cl(2)	2.3721(4)	Mn−N(3)	2.2681(12)
Mn−N(1)	2.2573(12)		
Cl(1)−Mn−Cl(2)	111.166(16)	Cl(2)−Mn−N(2)	104.55(3)
Cl(1)−Mn−N(1)	104.36(3)	Cl(2)−Mn−N(3)	102.61(3)
Cl(1)−Mn−N(2)	144.23(3)	N(1)−Mn−N(2)	71.98(1)
Cl(1)−Mn−N(3)	97.88(3)	N(1)−Mn−N(3)	141.86(4)
Cl(2)−Mn−N(1)	97.75(3)	N(2)−Mn−N(3)	71.86(4)

2, 0.3 × 0.5 × 0.5 mm for **3**, and 0.2 × 0.2 × 0.5 mm for **4** were selected. Diffraction data were collected on a Bruker SMART diffractometer with Mo Kα radiation. The crystallographic data are summarized in Tables 1−3. All calculations were effected using the SHELXTL computer program.[12] The full details of the X-ray structure determination can be found in the Supporting Information. Crystallographic data for the structural analysis have been deposited with the Cambridge Crystallographic Data Center, CCDC Nos. 233717−233720 for crystals **1** and **4**. Copies of the data may be obtained free of charge from The Director, CCDC, 12 Union Rd., Cambridge CB2 IEZ, U.K. (fax, +44-1223-336-033; e-mail, deposit@ccdc.cam.ac.uk; URL, www.ccdc.cam.ac.uk).

Results

Crystal Structure Determination. The crystal structures of [Mn(terpy)$(I)_2$] (**1**), [Mn(terpy)$(Br)_2$] (**2**), [Mn(terpy)$(Cl)_2$]·H_2O (**3**·H_2O), and [Mn(terpy)$(SCN)_2$] (**4**) have been determined by single-crystal X-ray crystallography. Table 1 gives the principal crystallographic data of the four complexes. Table 2 summarizes selected bond distances and angles for complexes **1**, **2**, and **4**, while Table 3 gives selected bond distances and angles for complex **3**. Figure 1 displays the structure of the four complexes.

Complexes **1**, **2**, and **4** present the trigonal bipyramidal geometry. The equatorial plane is defined by the two anions X (X = I^- , **1**; Br^-, **2**; SCN^-, **4**) and the central nitrogen atom of the terpy ligand (N(2)). The two distal nitrogen atoms of terpy (N(1) and N(1)#1) are located in the axial positions. These three complexes possess a C_2 axis passing through the manganese ion and the central nitrogen atom N(2) of terpy, implying the crystallographically equivalence of the two anions and the two distal nitrogens. Compared to the idealized trigonal bipyramid, the valency angles of the manganese atom show significant distortions. The spatially constrained nature of the tridentate terpy produces geometrical distortions manifested in the N(1)−Mn−N(1)#1 and N(2)−Mn−N(1) angles (Table 2). Thus, the distortions of the trigonal axis are similar for each complex with N(1)−Mn−N(1)#1 angles between 144.1(2)° and 145.33(13)° and reduced from the theoretical value of 180°. Similar deviations are found in [Mn(terpy)$(dmb)_2$] and $[Mn(terpy)_2]^{2+}$ complexes.[13] These deviations are larger than for other first-row transition-metal ions owing to the larger size of the Mn(II) ion. The equatorial plane in **1**, **2**, and **4** also shows significant distortions. In particular, the X−Mn−X#1 angles (between 104.09(14)° and 116.08(6)°) are smaller than the theoretical

(12) Sheldric, G. M. *SHELXTL-Plus, vers. 5.1 Structure Determination Software Programs*; Bruker-AXS Inc.: Madison, WI, 1998.

(13) (a) Erre, L. S.; Micera, G.; Garribba, E.; Bényei, A. C. *New J. Chem.* **2000**, *24*, 725. (b) Bhula, R.; Weatherburn, D. C. *Aust. J. Chem.* **1991**, *44*, 303. (c) Oshio, H.; Spiering, H.; Ksenofontov, V.; Renz, F.; Guetlich, P. *Inorg. Chem.* **2001**, *40*, 1143.

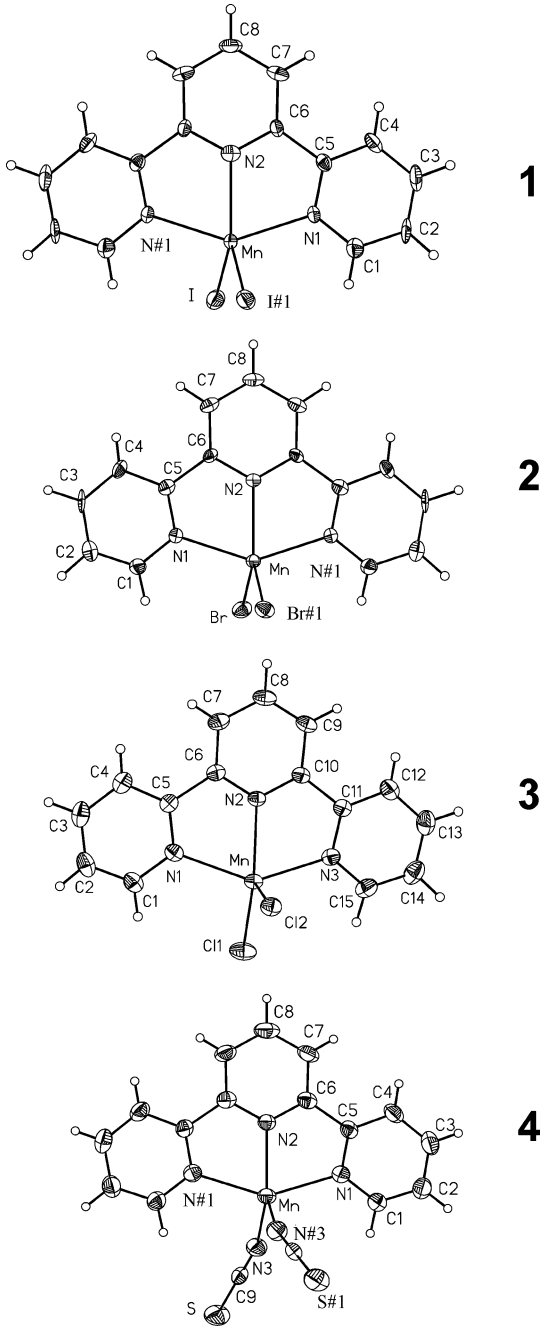

Figure 1. ORTEP diagrams showing the molecular structure of complexes **1**−**4**. Hydrogen atoms have been omitted for clarity.

value of 120°, while the other two angles N(2)−Mn−X of the equatorial plane are slightly higher (between 121.96(3)° and 127.95(7)°).

The structure of complex **3** is similar to that determined previously by Grirrane et al.[10] Complex **3** is better described as a distorted square pyramid with the basal positions occupied by the three nitrogen atoms of terpy, N(1), N(2), and N(3), and by the chloro atom Cl(1). The apical position is occupied by Cl(2). Compared to complexes **1**, **2**, and **4**, **3** presents this geometry since the N(2)−Mn−Cl(2) angle (104.55(3)°) is significantly smaller and the N(2)−Mn−Cl(1) angle (144.23(3)°) larger than those of the other systems (N(2)−Mn−N(X) = 122.85(3)°, 121.96(3)°, and 127.95(7)° for **1**, **2**, and **4**, respectively). Furthermore, the Mn−Cl(2) bond length (2.3721(4) Å) is longer than the Mn−Cl(1) bond length (2.3532(4) Å), while in **1**, **2**, and **4**, the two anions are equidistant. Five-coordinated Mn(II) complexes are usually characterized by a trigonal bipyramidal geometry, and the square pyramidal geometry has only been described in a few cases.[14] Compared to the idealized square pyramid, the valency angles in **3** show significant distortions. Among the four apical to basal angles, the Cl(2)−Mn−N(2) (104.55(3)°) and Cl(2)−Mn−N(3) (102.61(3)°) angles are close to the theoretical value of 104.1° for an idealized square pyramid, while Cl(2)−Mn−N(1) (97.75(3)°) and Cl(1)−Mn−Cl(2) (111.166(16)°) deviate by about 7° from this theoretical value. The large value of the Cl(1)−Mn−Cl(2) angle is due to the Cl(1)···Cl(2) repulsion. The steric requirements of the terpy ligand imply that the two angles N(1)−Mn−N(2) (71.98(1)°) and N(2)−Mn−N(3) (71.86(4)°) are smaller than the theoretical value of 86.6° while the other two angles Cl(1)−Mn−N(1) (104.36(3)°) and Cl(1)−Mn−N(3) (97.88(3)°) are larger. The Cl(1)−Mn−N(2) and N(1)−Mn−N(3) angles of 144.23(3)° and 141.86(4)°, respectively, also deviate from the theoretical value of 151.91°. The structure of **3** is comparable to that of [Mn(BBP)$(Cl)_2$][14a] (BBP = bis(benzylimidazole)pyridine). The valency angles and bond distances are closed, except that in [Mn(BBP)-$(Cl)_2$], the Mn−$N_{central}$ bond (2.267 Å) is longer than the Mn−N_{distal} distances (average 2.244 Å) (see below).

The Mn−N_{terpy} bond lengths are similar in the four complexes and independent of the nature of the anion bound to the Mn(II) ion. They are typical for terpy systems with the Mn−$N_{central}$ bond length smaller (2.233(7), 2.204(6), 2.2099(11), and 2.192(3) Å for **1**−**4**, respectively) than the Mn−N_{distal} bond length (average 2.240(6), 2.242(5), 2.2627-(76), and 2.241(3) Å for **1**−**4**, respectively). These values are comparable to those observed in [Mn(terpy)$(dmb)_2$] (Mn−$N_{central}$ = 2.226 Å and Mn−$N_{distal,av}$ = 2.279 Å) and in $[Mn(terpy)_2]^{2+}$ (Mn−$N_{central}$ = 2.190 Å, Mn−$N_{distal,av}$ = 2.248 Å).[13] This distortion, always observed in terpy complexes, is attributed to a more efficient overlap of the metal t_{2g} orbitals with π^* orbitals of the central pyridyl moiety compared to the distal pyridyl rings.

The Mn−X bond lengths are similar to those found in other Mn(II)−X complexes: 2.661 < Mn−I < 2.767 Å[15] (2.7200(9) Å for **1**), 2.490 < Mn−Br < 2.666 Å[15a,16] (2.5010(11) Å for **2**), 2.224 < Mn−Cl < 2.538 Å[14,15a,16d,17] (2.3532(4) Å (Cl(1)) and 2.3721(4) Å (Cl(2)) for **3**), and

(14) (a) Shuangxi, W.; Ying, Z.; Fangjie, Z.; Qiuying, W.; Liufang, W. *Polyhedron* **1992**, *11*, 1909. (b) Di Vaira, M.; Mani, F. *J. Chem. Soc., Dalton Trans*. **1990**, 191. (c) Ferrari, M. B.; Fava, G. G.; Pelizzi, P.; Tarasconi, P.; Tosi, G. *J. Chem. Soc., Dalton Trans*. **1987**, 227.

(15) (a) Turner, P.; Gunter, M. J.; Skelton, B. W.; White, A. H. *Aust. J. Chem*. **1998**, *51*, 853. (b) Aviles, T.; Carrondo, M. A. A. F. de C. T.; Piedade, M. F. M.; Teixeira, G. *J. Organomet. Chem*. **1990**, *388*, 143. (c) Hebendanz, N.; Köhler, F. H.; Müller, G. *Inorg. Chem.* **1984**, *23*, 3044.

(16) (a) Delaunay, J.; Hugel, R. P. *Inorg. Chem.* **1986**, *25*, 3957. (b) Butcher, R. J.; Sinn, E. *J. Chem. Soc., Dalton Trans.* **1976**, 1186. (c) Girolami, G. S.; Wilkinson, G. *J. Am. Chem. Soc.* **1983**, *105*, 6752. (d) Tajiri, Y.; Ichihashi, M.; Mibuchi, T.; Wakita, H. *Bull. Chem. Soc. Jpn.* **1986**, *59*, 1155.

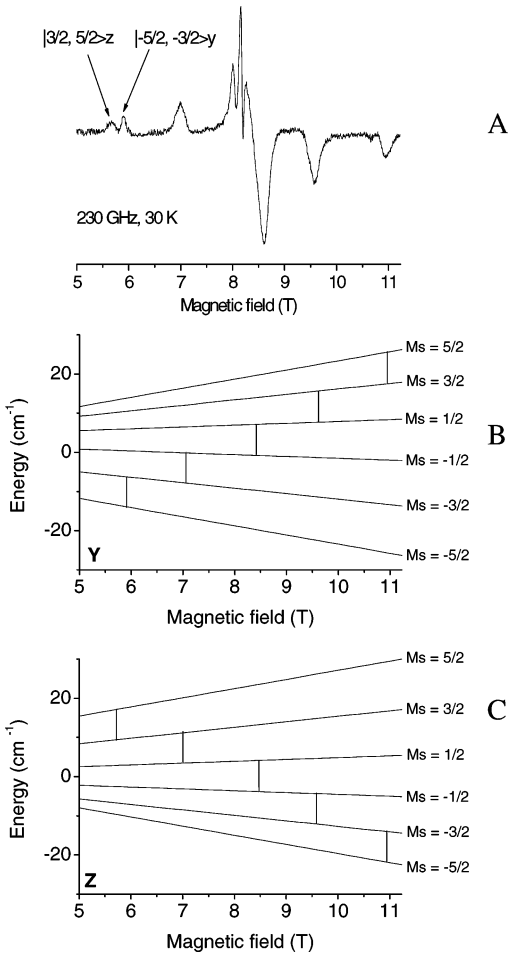

Figure 2. Energy vs field for the six levels arising from an $S = 5/2$ spin state using the parameters given below. The field is parallel to the molecular axis, along y (B) and along z (C). The observed resonances at 230 GHz are indicated by vertical bars. (A) Experimental powder HF-EPR spectra of complex **2** recorded at 230 GHz and at 30 K. The parameters used for the simulations are $D = +0.605(5)$ cm^{-1}, $E = 0.159(1)$ cm^{-1}, $g_x = 1.985(10)$, $g_y = 1.975(10)$, and $g_z = 1.965(10)$.

finally 2.067 < Mn−SCN < 2.185 Å[15a,18] (2.062(3) Å for **4**). The decrease of the Mn−X bond lengths in the order Mn−I > Mn−Br > Mn−Cl > Mn−NCS is obviously correlated with the electronegativity properties of the anions ($I^- < Br^- < Cl^- < SCN^-$).

Multifrequency EPR Study. The HF-EPR experiments were performed on polycrystalline powder pellets of complexes **1**−**4**. A multifrequency EPR study between 95 and 285 GHz was accomplished over a temperature range of 5−30 K.

Figures 2 and 3 display HF-EPR spectra recorded on complex **2** at 230 GHz ($g = 2$ at 8.21 T) and at different

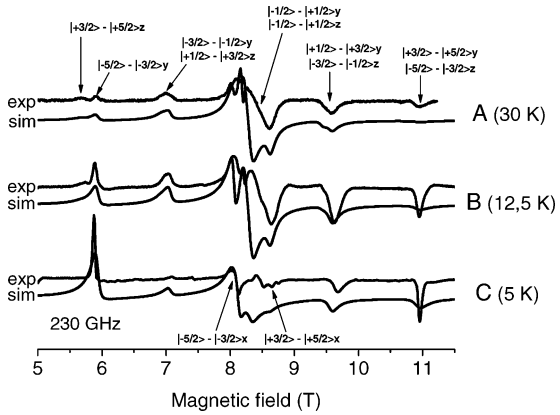

Figure 3. Experimental (exp) and simulated (sim)powder HF-EPR spectra of complex **2** recorded at 230 GHz and at three temperatures: 30 K (A), 12.5 K (B), and 5 K (C). The parameters used for the simulations are $D = +0.605(5)$ cm^{-1}, $E = 0.159(1)$ cm^{-1}, $g_x = 1.985(10)$, $g_y = 1.975(10)$, and $g_z = 1.965(10)$.

temperatures (5, 12.5, and 30 K). At this frequency, complete EPR spectra are obtained between 5.5 and 11.0 T. Since high-field-limit conditions are reached at this frequency ($D \ll g\beta B$), only lines originating from transitions that occur between two Zeeman levels by following the rules $\Delta M_s = \pm 1$ are observed. Because the experiments are carried out on neat powder samples, the observation of nuclear hyperfine splitting is avoided in the different electronic spin transitions.

In Figure 3, the effect of temperature on the EPR spectra is shown. At 5 K, only the lower M_s levels in energy are populated. Three significant lines are observed at 5.87, 8.10, and 10.95 T. When the temperature increases, the outer lines become less intense to the benefit of other lines at 7.00 and 9.67 T and around $g = 2$ appear or get more intense in agreement with the Boltzmann population of the M_s levels. From the 5 K spectrum, the sign as well as the magnitude of D can be afforded. Since the furthest transition (10.95 T) from the center of the spectrum (g around 2.00 for Mn^{2+}) is located in the high-field part, D is positive. This transition is associated with the $|5/2, -5/2\rangle \rightarrow |5/2, -3/2\rangle$ transition along the z axis with $D_{zz} > D_{xx}$ and D_{yy} and $D_{zz} + D_{xx} + D_{yy} = 0$ (with $D_{zz} = 2D/3$, $D_{xx} = (3E - D)/3$, and $D_{yy} = -(D + 3E)/3$). Its field difference from the central field of the spectrum is $|4D/g_z\beta|$, implying a D value of 0.68 T or 0.63 cm^{-1} (with $g_z = 2.00$ as a first approximation). A second transition observed at 9.67 T increases from 5 to 12.5 K in agreement with the Boltzmann population of the M_s levels. Thus, this transition is associated with the second transition of the quintet along z, $|5/2, -3/2\rangle \rightarrow |5/2, -1/2\rangle$. Furthermore, it is located at the expected field position of $|2D/g_z\beta|$ from the $|5/2, -5/2\rangle \rightarrow |5/2, -3/2\rangle$ transition along z, confirming our analysis.

The other 5 K spectra features are associated with x and y transitions. The 5.87 and 7.04 T lines are, respectively, assigned to the $|5/2, -5/2\rangle \rightarrow |5/2, -3/2\rangle$ and $|5/2, -3/2\rangle \rightarrow |5/2, -1/2\rangle$ y transitions. These attributes are confirmed thanks to the temperature effect on their relative intensity. In fact, the intensity of the first transition of the y quintet decreases from 5 to 12.5 K, whereas the second one increases. Along the x axis, it is more complicated to assign

(17) (a) Phillips, F. L.; Shreeve, F. M.; Skapski, A. C. *Acta Crystallogr.* **1976**, *B32*, 687. (b) Oki, R.; Bommarreddy, P. R.; Zhang, H.; Hosmane, N. *Inorg. Chim. Acta* **1995**, *231*, 109. (c) Lah, M. S.; Chun, H. *Inorg. Chem.* **1997**, *36*, 1782. (d) Goodson, P. A.; Oki, A. R.; Hodgson, D. J. *Inorg. Chim. Acta* **1990**, *177*, 59. (e) McCann, S.; McCann, M.; Casey, R. M. T.; Jackman, M.; Devereux, M.; McKee, V. *Inorg. Chim. Acta* **1998**, *279*, 24.

(18) (a) Mikuriya, M.; Hatano, Y.; Asato, E. *Bull. Chem. Soc. Jpn.* **1997**, *70*, 2495. (b) Oshio, H.; Ino, E.; Mogi, I.; Ito, T. *Inorg. Chem.* **1993**, *32*, 5697. (c) Holleman, S. R.; Parker, O. J.; Breneman, G. L. *Acta Crystallogr.* **1994**, *C50*, 867.

Table 4. Electronic Parameters and Coordination Number for Complexes **1**−**4** and Mn(II) Complexes Described in the Literature

compound	coord no.	D (cm^{-1})	E (cm^{-1})	$\lvert E/D\rvert$	g_x	g_y	g_z
1	5	+1.000(5)	0.19(1)	0.19	1.98(2)	1.99(2)	1.97(2)
$Mn(PPhO)_2(I)_2$[a]	4	0.906	0.223	0.246	2.0039	2.0039	2.0039
$Mn(pic)_4(I)_2$[b]	6	0.999	0.005	0.005	2.001	2.001	2.001
$Mn(phen)_2(I)_2$[b]	6	0.590	0.145	0.246	2.008	2.008	2.008
$Mn(pyr)_4(I)_2$[c]	6	0.932	0.0196	0.021	2.00	2.00	2.00
$Mn(N_2H_4)_2(I)_2$[d]	6	1.21	0.023	0.019	2.00	2.00	2.00
2	5	+0.605(5)	0.159(1)	0.26	1.985(10)	1.985(10)	1.985(10)
$Mn(PPhO)_2(Br)_2$[a]	4	0.507	0.134	0.263	1.9985	1.9985	1.9985
$Mn(pic)_4(Br)_2$[b]	6	0.626	0.003	0.005	2.002	2.002	2.002
$Mn(phen)_2(Br)_2$[b]	6	0.359	0.074	0.21	2.002	2.002	2.002
$Mn(pyr)_4(Br)_2$[c]	6	0.590	0.0032	0.0054	2.00	2.00	2.00
$Mn(N_2H_4)_2(Br)_2$[d]	6	0.71	0	0	2.00	2.00	2.00
3	5	−0.26(2)	0.075(5)	0.29	1.994(5)	2.010(7)	2.025(5)
$Mn(PPhO)_2(Cl)_2$[a]	4	0.165	0.045	0.273	2.0000	2.0000	2.0000
$Mn(pic)_4(Cl)_2$[b]	6	0.186	0	0	2.004	2.004	2.004
$Mn(phen)_2(Cl)_2$[b]	6	0.124	0.005	0.04	2.000	2.000	2.000
$Mn(pyr)_4(Cl)_2$[c]	6	0.208	0.000	0	2.00	2.00	2.00
$Mn(N_2H_4)_2(Cl)_2$[d]	6	0.29	0.0044	0.015	2.00	2.00	2.00
4	5	−0.30(1)	0.050(5)	0.17	1.99(2)	1.97(2)	1.97(1)
$Mn(pyr)_4(SCN)_2$[c]	6	0.01	0.002	0.20	2.00	2.00	2.00

[a] Reference 7b (PPhO = triphenylphosphine oxide). [b] Reference 7a (pic = γ-picoline, phen = *o*-phenanthroline). [c] Reference 6f (pyr = pyridine) (for the Br, Cl, and SCN complexes, Mn(II) in Co(II); for I complex, Mn(II) in Fe(II)). [d] Reference 6e (hyd = N_2H_4 ; Mn(II) in Zn).

the different transitions since they are less resolved and located at around $g = 2$.

In the case of a pure axial system, the *x* and *y* transitions are located at $\pm 2D$ and $\pm D$ from the center of the spectrum ($g = 2$) and at $g = 2$. For a pure rhombic system, the *y* transitions are located at $\pm 4D$ and $\pm 2D$ from the center of the spectrum ($g = 2$) and at $g = 2$, and the *x* transitions are all located at $g = 2$. Since the $|5/2, -5/2\rangle \rightarrow |5/2, -3/2\rangle$ *x* transition is located at 8.1 T (close to $g = 2$), it is the signature of a quasi-rhombic system, implying an E/D value close to 1/3. An estimation of E can be done from the resonance field difference of the two subsequent y transitions, which corresponds to $|(3E - D)/g_y\beta|$. This implies an E value of 0.163 cm^{-1}.

At 30 K, all Zeeman levels are populated as shown in Figure 2, and all transitions have been assigned. The energy diagrams of the Zeeman levels as a function of the field are shown along the *y* and *z* axes to validate our assignment. The outer lines corresponding to the transitions that occur between the $\pm 5/2$ and $\pm 3/2$ Zeeman levels along *y* and *z* appear as doublets. This is also the signature of a quasi-rhombic EPR spectrum of Mn(II) recorded at high temperature, with the *y* and *z* transitions located at close resonance fields. This splitting is less clear in the intermediate lines at around 7.0 and 9.7 T.

As hyperfine interactions are absent in the experimental data, the spin Hamiltonian (eq 2) that describes our system is simplified compared to eq 1.

$$H = \beta BgS + D[S_z^2 - (1/3)S(S+1)] + E(S_x^2 - S_y^2) \quad (2)$$

The HF-EPR spectra were simulated using a full-matrix diagonalization procedure of the spin Hamiltonian (eq 2). The best simulation of the experimental data (Figure 3) was obtained using the following spin Hamiltonian parameters reported in Table 4: $D = +0.605(5)$ cm^{-1}, $E = 0.159(1)$ cm^{-1}, $g_x = 1.985(10)$, $g_y = 1.975(10)$, $g_z = 1.965(10)$ cm^{-1}.

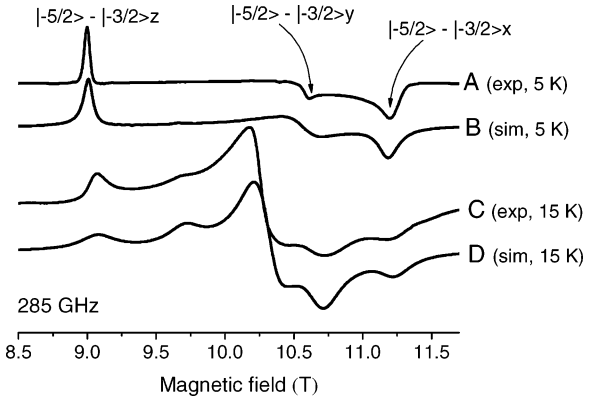

Figure 4. Experimental (exp) and simulated (sim)powder HF-EPR spectra of complex **4** recorded at 285 GHz and at two temperatures: 5 K (A, B) and 15 K (C, D). The parameters used for the simulations are $D = -0.30(1)$ cm^{-1}, $E = 0.050(5)$ cm^{-1}, $g_x = 1.99(2)$, $g_y = 1.97(2)$, and $g_z = 1.97(1)$.

It can be noticed that these parameters are close to those estimated from a simple view of the experimental data. These spin Hamiltonian parameters likewise simulate successfully HF-EPR spectra recorded at all temperatures and frequencies.

The same analysis was performed for complexes **1**, **3**, and **4**, and the corresponding spin Hamiltonian parameters are reported in Table 4. All studies have been done at several frequencies (95−285 GHz) to unambiguously confirm the determined spin Hamiltonian parameters. The magnitude of D is directly related to the total width of the spectra of about 7.5 T for **1** ($D = +1.000(5)$ cm^{-1}), 5.5 T for **2** ($D = +0.605(5)$ cm^{-1}), 2.2 T for **3** ($D = -0.26(2)$ cm^{-1}), and 2.5 T for **4** ($D = -0.30(1)$ cm^{-1}) (see below).

Figure 4 shows the 285 GHz EPR spectra recorded on a powder sample of **4** at 5 and 15 K. The EPR signature of this complex is different from that of **2** (Figures 2 and 3) since the total width of the spectra is smaller. This is correlated with the magnitude of D. However, the line width of the transitions is similar in both complexes at 5 K. This implies that, for systems with small D values, the spectra

will be less resolved. This is the case for **4**. Furthermore, for **4**, the line width increases with an increase of the temperature due to different relaxation properties of **4** compared to the other three complexes. At 15 K, due to the broadening of the transitions, only five features are well resolved, from which the spin Hamiltonian parameters cannot be unambiguously determined. Thanks to the 5 K spectrum, the sign and the magnitude of D can be measured. D is negative since the $|5/2, -5/2\rangle \rightarrow |5/2, -3/2\rangle$ transition along z (9.0 T) is located in the low-field part of the spectrum. Its magnitude is estimated to be 0.28 cm^{-1} ($|4D/g_z\beta|$ from $g = 2$, 10.2 T at 285 GHz). E can be estimated from the other two 5 K features associated with the $|5/2, -5/2\rangle \rightarrow |5/2, -3/2\rangle$ transition along x (11.2 T) and y (10.56 T). For instance, the field difference between them is equal to $|12E/g_{x,y}\beta|$ if we consider at a first approximation that g_x and g_y are equal to 2.0. Thus, E is estimated to be 0.05 cm^{-1}. The agreement between those estimations and the spin Hamiltonian parameters determined from simulations given in Table 4 is good, demonstrating the importance of the low-temperature HF-EPR experiments.

Discussion

Very few five-coordinated Mn(II) complexes[6b] have been studied by EPR, and the present study is the first one in which an investigation of a series of five-coordinated Mn(II) compounds is undertaken. Therefore, we proposed to discuss here some of the electronic properties of this series and to compare them with other analogous series of four- or six-coordinated Mn(II) complexes previously described.[6e,f,7]

First, we will discuss the correlation between the structure and the spin Hamiltonian parameters found for our series of complexes. The resolution of the structures by X-ray diffraction shows that complexes **1**, **2**, and **4** possess a distorted trigonal bipyramidal geometry, while **3** is too distorted to be considered in this geometry and is better described as a distorted square pyramid. Another significant difference between the four complexes is the Mn−X bond lengths directly correlated with the electronegativity of the anions X. Otherwise, the rigidity of the terpy ligand leads to similar structural data for all complexes concerning the $Mn-N_{terpy}$ distances and the N(2)−Mn−N(1), N(3), or N(1)−Mn−N(1)#1, N(3), angles.[13]

The electronic properties of these complexes were investigated by HF-EPR spectroscopy. As observed in the previous HF-EPR studies performed on mononuclear Mn(II) complexes,[7] we found that the zfs parameters can be easily estimated directly from the HF-EPR spectra. However, in these previous studies, the sign of D was not determined since the experiments were performed at room temperature.[7] In this study, we determined the sign of D by recording spectra at low temperature. Complexes **1** and **2** have a positive D value, and complex **4** has a negative one. It appears that the sign of D can be correlated with the crystallographic structures of the complexes. Complexes **1** and **2** present axially compressed trigonal bipyramidal configurations in which the axial bonds ($Mn-L_{ax} = 2.240(6)$ Å (**1**) and 2.242(5) Å (**2**)) are significantly shorter than the equatorial ones ($Mn-L_{eq,av} = 2.557(281)$ Å (**1**) and 2.402(171) Å (**2**)), while **4** can be described as an elongated trigonal bipyramid ($Mn-L_{ax} = 2.241(3)$ Å; $Mn-L_{eq,av} = 2.1053(751)$ Å). Thus, a positive D corresponds to a trigonal compression geometry of the complex and a negative D to an elongation. In the case of complex **3**, the high E/D value of 0.29 (close to the limit value of 1/3) causes the determination of the sign of D to be less obvious. However, from the low-temperature HF-EPR spectra, the best simulation is obtained with a negative D. Thus, the elongated square pyramid observed for **3**, with the axial bond lengths longer ($Mn-Cl(2) = 2.3721(4)$ Å) than the equatorial ones ($Mn-L_{eq,av} = 2.2721(596)$ Å), may be correlated with the negative sign of D.

In the literature, it has been shown that the sign of D can be correlated with the sense of the trigonal distortion in the special case of six-coordinated Mn(II) complexes with D_{3d} symmetry.[19] A positive D corresponds to trigonal compression and a negative D to trigonal elongation. For other geometries and symmetries, to our knowledge, such a correlation has not been investigated. Furthermore, the sign of D is rarely determined and only for systems with small D values (<0.1 cm^{-1}).[19]

In Table 4, we report the spin Hamiltonian parameters for complexes **1**−**4** along with those of the other related manganese (II) complexes previously published. D is comparable in the different complexes containing the same anion ($X = I^-$, Br^-, Cl^-), except for the *o*-phenanthroline compounds.[7a] $|D|$ is between 0.9 and 1.2 cm^{-1} for the iodo complexes, between 0.5 and 0.7 cm^{-1} for the bromo complexes, and between 0.16 and 0.30 cm^{-1} for the chloro complexes. In the case of the *o*-phenanthroline series,[7a] the decrease of D from the iodo (0.590 cm^{-1}) to the chloro (0.124 cm^{-1}) complexes is also observed, but the magnitudes of D are significantly lower than for the other systems. The authors have suggested[7b] that this difference is due to the *trans* arrangement of the anions in the *o*-phenanthroline complexes versus a *cis* arrangement in the γ-picoline complexes.

For complexes with thiocyano anions, the magnitude of D was only determined for **4** and $[Mn(pyr)_4(SCN)_2]$.[6f] No conclusion can be drawn due to the important discrepancy observed between the two D values of these complexes, respectively equal to 0.30(1) and 0.01 cm^{-1}.

D is mostly governed by the nature of the anionic ligand since the ligand field strength of the anion is much smaller than that of the neutral ligands. Indeed, as was previously demonstrated (Table 4), the magnitude of D of the iodo, bromo, thiocyano, and chloro complexes is inversely proportional to the ligand field strength of each anion (Δ_o: $I^- < Br^- < SCN^- < Cl^-$). This is confirmed for complexes **1**−**4** with D increasing in the order $Cl^- < SCN^- < Br^- < I^-$, from 0.26 to 1 cm^{-1}.

As can be seen, in the presence of ligands characterized by a weak ligand field, the coordination number of the manganese ion cannot be correlated with D. Nevertheless,

(19) (a) Hempel, J. C. *J. Chem. Phys.* **1976**, *64*, 4307 (b) Palmer, R. A.; Yang, M. C.-L.; Hempel, J. C. *Inorg. Chem.* **1978**, *17*, 1200.

in the case of Mn(II) metalloenzymes in which the coordination shell is formed by only strong-field ligands such as N or O ligands, the coordination number of the manganese ion can be afforded as a function of the magnitude of D.[5a,b]

The E/D ratio is significantly affected by the geometry and the coordination number of the complexes as can be seen in Table 4. It varies from pure axial systems ($E/D = 0$) to close rhombic ones ($E/D = 1/3$). In all cases, the rhombicity seems to mostly depend on the nature of the neutral ligand. For octahedral systems, with monodentate ligands such as pyridine or γ-picoline, the systems are axial or quasi-axial except for the thiocyano complex, for which the D and E were not accurately determined.[6f,7a] For bidentate ligands such as *o*-phenanthroline, the constraint due to the ligand provokes an increase of the E/D values higher than 0.2 cm^{-1}, except for the chloride complex.[7a] In the tetrahedral series, the E/D values are higher than 0.2 cm^{-1} as predicted for tetrahedral (C_{2v}) complexes.[7b] In our five-coordinated series, the rigidity of the terpy is at the origin of strong distortions around the metallic ion characterized by E/D between 0.19 and 0.29 cm^{-1}. The E/D ratio is also affected by the nature of the anions Cl^-, Br^-, and I^-, but no conclusion can be drawn. Indeed, in the case of octahedral complexes, E/D decreases from the iodo complex to the chloro one,[7a] while for our series and for the tetrahedral systems, E/D increases from the iodo complex to the chloro one.[7b]

The g values are between 1.970 and 2.025. Complex **3** has the greatest g values and at the same time the smallest D value. This phenomenon contradicts simple ligand field theory predictions. However, when one considers the whole literature on mononuclear Mn(II) complexes, no correlation between g and D can be established from the experiments. As an example, the same observation is found for the pic series.[7a]

Conclusion

We have demonstrated here the application of HF-EPR to properly investigate the electronic properties of distorted five-coordinate Mn(II) complexes. In particular, we have shown the importance of the low-temperature experiments to determine the sign of the axial zfs parameter D, which seems to be directly correlated with the geometry around the manganese ion. In the case of five-coordinated systems, an axially elongated trigonal bipyramid is associated with a negative sign of D, while a compression is characterized by a positive D. The coordination number of the Mn(II) cannot be correlated with D since its magnitude mostly depends on the ligand field strength of the anionic ligand.

Acknowledgment. I. R. thanks the CNRS for financial support.

Supporting Information Available: X-ray crystallographic details for complexes **1** (Table S1), **2** (Table S2), **3** (Table S3), and **4** (Table S4) in CIF format. This material is available free of charge via the Internet at http://pubs.acs.org.

IC049650K